

Changes in climate extreme events in China associated with warming

Huopo Chen^{a,b*} and Jianqi Sun^a

^a Nansen-Zhu International Research Centre, Institute of Atmospheric Physics, Chinese Academy of Sciences, Beijing, China

^b Collaborative Innovation Center on Forecast and Evaluation of Meteorological Disasters, Nanjing University of Information Science & Technology, China

ABSTRACT: The science that humans are the cause of global warming, and that the associated climate change would lead to serious changes in climate extreme events, food production, freshwater resources, biodiversity, human mortality, etc. is unequivocal. After several political negotiations, a 2 °C warming has been considered to be the benchmark for such damaging changes. However, an increasing amount of scientific research indicates that higher levels of warming are increasingly likely. What would the world be like if such higher levels of warming occurred? This study aims to provide information for better politically driven mitigation through an investigation of the changes in temperature- and precipitation-based extreme indices using CMIP5 (coupled model intercomparison project phase 5) simulations of a warming of 1, 2, and 3 °C in China. Warming simulations show more dramatic effects in China compared with the global average. In general, the results show relatively small change signals in climate extreme events in China at 1 °C, larger anomalies at 2 °C, and stronger and more extended anomalies at 3 °C. Changes in the studied temperature indices indicate that warm events would be more frequent and stronger in the future, and that cold events would be reduced and weakened. For changes in the precipitation indices, extreme precipitation generally increases faster than total wet-day precipitation, and China will experience more intensified extreme precipitation events. Furthermore, the risk of flooding is projected to increase, and the dry conditions over northern China are projected to be mitigated. In certain regions, particularly Southwest China, the risks of both drought and flood events would likely increase despite the decreased total precipitation in the future. Uncertainties mainly derived from inter-model and scenario variabilities are attached to these projections, but a high model agreement can be generally observed in the likelihood of these extreme changes.

KEY WORDS 2 °C warming; climate extreme events; projection; CMIP5; ETCCDI; uncertainty; China

Received 24 March 2014; Revised 13 August 2014; Accepted 19 August 2014

1. Introduction

Future changes in climate extreme events, including extreme temperature and precipitation events, are of particular relevance to society and ecosystems due to the potentially severe impacts of such changes, as emphasized in the Special Report on Extreme Events (SREX) of the Intergovernmental Panel on Climate Change (IPCC, 2012). These changes are particularly concerning for some continental regions (e.g. China) that generally have a high vulnerability to climate change and relatively low adaptive capacity. Correspondingly, the demand for consistent and robust projections of future changes in climate extremes has rapidly increased over the past several years.

To facilitate the investigation of observed and projected changes in climate extremes, much effort has been devoted to develop valuable indices that focus on the extremes, such as the 27 climate extreme indices produced

by the Expert Team on Climate Change Detection and Indices (ETCCDI), which generally describe moderate extreme events with a reoccurrence time of 1 year or less (Zhang *et al.*, 2011). These indices have been widely used to analyse the climate extreme changes in historical records (e.g. Alexander *et al.*, 2006; Donat *et al.*, 2013) as well as in future climate projections (e.g. Orlowsky and Seneviratne 2012; Chen *et al.*, 2014; Sillmann *et al.*, 2013). Most importantly, these 27 ETCCDI climate extreme indices have been calculated based on the CMIP3 (coupled model intercomparison project phase 3; Meehl *et al.*, 2007) and CMIP5 (Taylor *et al.*, 2012) simulations conducted in a previous study (Sillmann *et al.*, 2013) and are freely shared with all researchers around the world. Compared with CMIP3, some substantial improvements in CMIP5 can be observed, and a new set of emission scenarios is used (Moss *et al.*, 2010; Taylor *et al.*, 2012). Thus, the analyses in this study of the future changes in climate extremes are mainly focused on the CMIP5 simulations.

Dominated by monsoon variability, the climate in China affects approximately one fifth of the world's population, which makes the robust projection of future climate changes vital to allow for better mitigation planning at the

* Correspondence to: H. Chen, Nansen-Zhu International Research Centre (NZC), Institute of Atmospheric Physics, Chinese Academy of Sciences, PO Box 9804, Beijing 100029, China.
E-mail: chenhuopo@mail.iap.ac.cn

national level. Such projections are available in China from both CMIP3 and CMIP5 simulations (e.g. Xu *et al.*, 2007, 2009; Chen and Sun, 2009, 2013; Jiang *et al.*, 2009; Xu *et al.*, 2009, 2010; Ma *et al.*, 2012; Xu and Xu, 2012a, 2012b; Zhang and Sun, 2012; Chen, 2013; Jiang and Tian, 2013; Lang and Sui, 2013). For example, a significant increase in interannual variability of summer precipitation can be observed over the East Asian monsoon areas in this century (Lu and Fu, 2010). Associated with this increase, the events related to precipitation will tend to be much more extreme (Chen *et al.*, 2012). Floods and droughts will be more frequent and stronger in some regions of China (Chen *et al.*, 2013). In addition, the intense snowfall events will decrease over southern China, but they initially increase and subsequently decrease over northern China (Sun *et al.*, 2010). These changes exhibit significant agreement with the simulations from regional climate models (RCMs), but there are more local, small-scale details provided by the high-resolution RCMs (Gao *et al.*, 2001, 2002, 2011, 2012a, 2012b; Xu *et al.*, 2013). These results have been well summarized by a previous review (Wang *et al.*, 2012).

Recently, the newly released IPCC Fifth Assessment Report (AR5) indicated that the average global surface air temperature warmed by 0.85°C ($0.65\text{--}1.06^{\circ}\text{C}$) over the 1880–2012 period. Many climate-change impacts have already started to emerge due to this rapid warming. The report further indicates that, even with full implementation of the current mitigation commitments and pledges, warming is likely to exceed 2°C relative to the present level (IPCC, 2013). What the world would be like if it warmed by 2°C and how to avoid that change have become central issues for scientists and for climate-change negotiators worldwide. Thus, research on the climate changes associated with increasing temperature has begun, and it shows that some of the changes that are projected to occur with a 2°C increase would have serious implications (e.g. Meinshausen *et al.*, 2009; Guiavarch and Hallegatte, 2011; Rogelj *et al.*, 2011; van Vuuren *et al.*, 2011); in addition, even larger shifts would accompany a 4°C increase (e.g. World Bank Group, 2012; James and Washington, 2013). Some researchers have investigated how China's climate will change in the future (Jiang *et al.*, 2009; Jiang and Fu, 2012; Zhang, 2012; Lang and Sui, 2013); however, the implications of rising temperature (e.g. by 1, 2, or 3°C) for climate extreme events in China have not been investigated.

Despite substantial improvements in climate models in recent years, projections are still uncertain due to the complex climate systems, which are poorly understood and inadequately modelled. Different emission scenarios, physical feedbacks, the carbon cycle, boundary and initial conditions, and other structural uncertainties are the main sources for the projection uncertainty (Knutti, 2008; Knutti *et al.*, 2008). These sources are generally classified into three types: inter-model variability, internal variability, and scenario uncertainty. Recent studies indicate that for the temperature and precipitation projections from a global perspective, internal variability is the dominant

source of uncertainty for projection of the near future, and inter-model variability is the dominant source of uncertainty for projection at the end of this century. However, the scenario contribution is small or even negligible, except for the regions close to the poles for the end of this century (Hawkins and Sutton, 2009, 2011). How do these sources perform in the regional scale? Their roles in the climate extreme projections in China will be further discussed.

The performance of the CMIP5 model in simulating climate extremes in China has been evaluated (H. P. Chen and J. Q. Sun, pers. comm.). The results indicate that most CMIP5 models can reasonably reproduce the spatial and trending patterns of the temperature-based extremes in China. However, there are also some discrepancies due to the cold biases in the model simulations. For example, overestimation is visible for frost days (FD) and ice days (ID), but underestimation is clear for warm events, such as summer days (SU). In addition, most CMIP5 models generally show strong performances in simulating the precipitation-based extremes but generally with relatively lower accuracy than for temperature-based simulations. The comparison of CMIP5 with CMIP3 further illustrates that the model spread for most extremes is reduced in CMIP5 despite a larger number of models participating in CMIP5. On the basis of the previous study, the purpose of this paper is to document the changes in climate extremes in China under different temperature increases, concurrently with the quantification of the associated projection uncertainty using CMIP5 simulations. Accordingly, the paper is organized as follows. We briefly describe the data sets and methods in Section 2. In Section 3, we provide the timing of global warming and the warming in China. The main results for the climate extreme changes on the basis of temperature and precipitation indices are presented in Section 4. A summary of the main findings and concluding remarks are given in Section 5.

2. Data and methods

To derive the global and regional mean temperature changes, monthly surface air temperature data are selected from the CMIP5 multi-model data set, which are archived at the website of the Earth System Grid (ESG) gateway hosted by the PCMDI (Program for Climate Model Diagnosis and Intercomparison). The 27 ETCCDI indices across CMIP5 ensembles that are calculated from the daily minima and maxima of near-surface temperature and daily precipitation amounts are provided by Sillmann *et al.* (2013) and available at <http://www.cccma.ec.gc.ca/data/climdex/climdex.shtml>. For the multi-model analysis in this paper, we re-gridded these indices and monthly temperature data to a common $1.5^{\circ} \times 1.5^{\circ}$ grid using a first-order conservative remapping procedure. The topographical adjustment is implemented for the re-gridded monthly temperature due to the different resolutions between the models and the target grids.

Compared with CMIP3, one important improvement is that CMIP5 provides four radiative forcing trajectories in the RCPs (representative concentration pathways) that

Table 1. List of the CMIP5 models used in this study.

	Model	Institute/country	Spatial resolution (Lon × Lat ~Levels)
1	BCC-CSM1.1	Beijing Climate Center, China Meteorological Administration, China	2.784° × 2.8125° L26
2	BNU-ESM	Beijing Normal University, China	2.784° × 2.8125° L26
3	CanESM2	Canadian Centre for Climate Modelling and Analysis, Canada	2.784° × 2.8125° L35
4	CCSM4	National Center for Atmospheric Research (NCAR), USA	0.942° × 1.25° L26
5	CNRM-CM5	Centre National de Recherches Meteorologiques, Meteo-France, France	1.397° × 1.406° L31
6	CSIRO-MK3.6.0	Australian Commonwealth Scientific and Industrial Research Organization, Australia	1.861° × 1.875° L18
7	FGOALS-g2	Institute of Atmospheric Physics, Chinese Academy of Sciences, China	2.8125° × 2.8125° L26
8	GFDL-ESM2G	Geophysical Fluid Dynamics Laboratory, USA	2.0225° × 2.5° L24
9	GFDL-ESM2M	Geophysical Fluid Dynamics Laboratory, USA	2.0225° × 2.5° L24
10	HadGEM2-ES	Met Office Hadley Centre, UK	1.25° × 1.875° L40
11	IPSL-CM5A-LR	Institut Pierre-Simon Laplace, France	1.895° × 3.75° L39
12	IPSL-CM5A-MR	Institut Pierre-Simon Laplace, France	1.268° × 2.5° L39
13	MIROC5	Atmosphere and Ocean Research Institute (AORI), National Institute for Environmental Studies (NIES), Japan Agency for Marine-Earth Science and Technology (JAMSTEC), Japan	1.397° × 1.406° L40
14	MIROC-ESM	AORI, NIES, JAMSTEC, Japan	2.784° × 2.8125° L80
15	MIROC-ESM-CHEM	AORI, NIES, JAMSTEC, Japan	2.784° × 2.8125° L80
16	MPI-ESM-LR	Max Planck Institute for Meteorology, Germany	1.861° × 1.875° L47
17	MPI-ESM-MR	Max Planck Institute for Meteorology, Germany	1.861° × 1.875° L95
18	MRI-CGCM3	Meteorological Research Institute, Japan	1.119° × 1.125° L48
19	NorESM1-M	Norwegian Climate Centre, Norway	1.895° × 2.5° L26

include new socioeconomic data, emerging technologies, and observed environmental factors (Moss *et al.*, 2010). Here, 19 CMIP5 models (Table 1) are analysed, which show that the climate extreme indices are available for three RCP scenarios (RCP2.6, 4.5, and 8.5).

The climate extreme changes are calculated as the differences between the future period and the present-day period (1986–2005) from the multi-model ensemble (MME) results, such that the MME performance is expected to outperform individual models in the case of present-day climate simulations over most regions (Jiang *et al.*, 2005). The MME is here defined as the median value of all the models, rather than the mean value, to guard against models with unusually large errors unduly influencing the results. The model agreement is first considered to be the significance of projected changes that are consistent with the likelihood levels in IPCC reports. Only the signals of ‘likely’ (more than 66% of the models agree on the sign of the change) and ‘very likely’ changes (at least 90% of the models agree on the sign of the change) are presented for the extreme indicators in China. The interquartile model range, i.e. the range between the 25th and 75th percentiles of the model ensemble, is also used to represent the confidence level when analysing the temporal evolution of such indices. To further quantify the uncertainty of the projected changes, the method proposed by Hawkins and Sutton (2009, 2011) is used here to separate the sources of uncertainty, including the

inter-model, internal, and scenario variabilities. First, each individual projection is fit, using ordinary least squares, with a fourth-order polynomial over the target period. Then, the inter-model variability, i.e. the variability due to different models producing somewhat different changes in the climate in response to the same radiative forcing, is considered to be the multi-scenario mean of the variances in the different model projection fits. The internal variability of each model is estimated from the multi-model mean of the variances of the residuals from the fits. The scenario uncertainty is simply the variance of the multi-model means for the three scenarios. The sum of these three components is taken to be the total uncertainty for the projection. More detailed information about this method can be found in the studies by Hawkins and Sutton (2009, 2011). In addition, to improve the readability of this study, a map of the region divisions in China is provided in Figure 1 as referenced in the following discussions.

3. Timing of global and regional warming

The spatially weighted averages of annual global temperature anomalies are first smoothed using an 11-year low-pass filtering method to eliminate interannual variability for each model and each scenario. All of the models project increasing global temperature in the RCP scenarios, and the median ensemble means show the largest

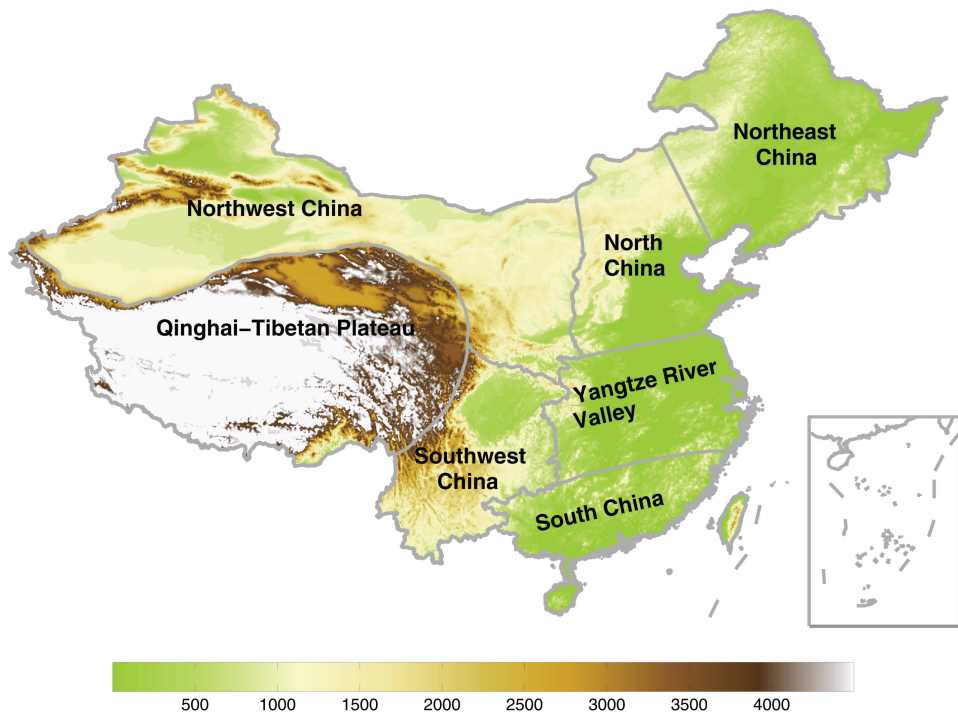


Figure 1. Plots of the regions in China referred to in this study. Shading indicates the topography. The inserted box represents the region's extent that has been labelled in the figure. Units: m.

increasing trend in RCP8.5 and the smallest increasing trends in RCP2.6 (Figure 2(a)). For the same radiative forcing scenario, the different models show different rates of warming, leading to a variation in the number of models at which the temperature exceeds specific thresholds. For example, there are 19 models that can reach a temperature threshold of 1, 2, and 3 °C in RCP8.5, ten models that can reach 4 °C and four models that can reach 5 °C; in RCP4.5, there are 19 models that can reach 1 °C and 9 models that can reach 2 °C, but none that reach 3 °C; and in RCP2.6, 13 models can reach 1 °C but no model can reach 2 °C. In addition, the year at which the models exceeded a specific temperature threshold varies among the models. For example, the timing of a 2 °C warming has a range of 2055–2099 in RCP4.5 and 2045–2072 in RCP8.5. From the median ensemble results, the global temperature increase surpassed 1, 2, and 3 °C in the years 2034, 2058, and 2079, respectively, in RCP8.5; a 1 °C warming occurred in the year 2038 for RCP4.5 and in 2042 for RCP2.6.

The projected change in the spatially weighted temperature average is also calculated for China. China warmed more than the global average, with larger warming trends observed in all the scenarios (Figure 2(b)). For example, the global annual temperature is projected to increase by 1 °C and the regional annual temperature is projected to increase by 1.7 °C in China in the RCP8.5 scenario; likewise, the annual temperature increases by 2 °C globally and 3.1 °C in China, and by 3 °C globally and 4.1 °C in China. The highest increases are generally found in the arid and semi-arid regions over northern China. Accordingly, the date of warming by 1, 2, and 3 °C occurs

much earlier in China than in the global averages, leading by approximately 1–2 decades. The years of an average annual temperature increase by 1, 2, and 3 °C in China are 2020, 2041, and 2057 in RCP8.5, respectively; there is an increase by 1 °C in 2027 and 2 °C in 2057 in RCP4.5; and there is an increase by 1 °C in 2023 in RCP2.6. These years are obtained from the results after an 11-year low-pass filtering process, and thus they are taken to be the central time-points for the calculation of a 20-year climatic mean for each extreme index in this study. In addition, all of the models project a temperature increase exceeding 4 °C in China in the RCP8.5 scenario, and 16 models project an increase of over 5 °C.

The IPCC report has suggested that annual surface-temperature increases of 1, 2, and 3 °C above the present level would lead to irreversible or dangerous changes in the climate system, food production, freshwater resources, biodiversity, human mortality, etc. (IPCC, 2012). Furthermore, the warming in China is reported to be much stronger and faster than the global pattern, leading to greater risks to society and ecosystems from regional warming. Thus, climate extreme changes will be evaluated in the following section by considering a regional warming of 1, 2, and 3 °C in China. The change signal is defined as the difference between the reference period and each of 20-year-sample climatology centred at the timing of a warming by 1, 2, and 3 °C. Although the annual temperature increase in China is projected to exceed 4 or 5 °C in the RCP8.5 scenario, the climate extreme changes at these warming levels will not be repeatedly discussed because the changes will be similar to those that occur with a warming of 3 °C but with greater magnitude.

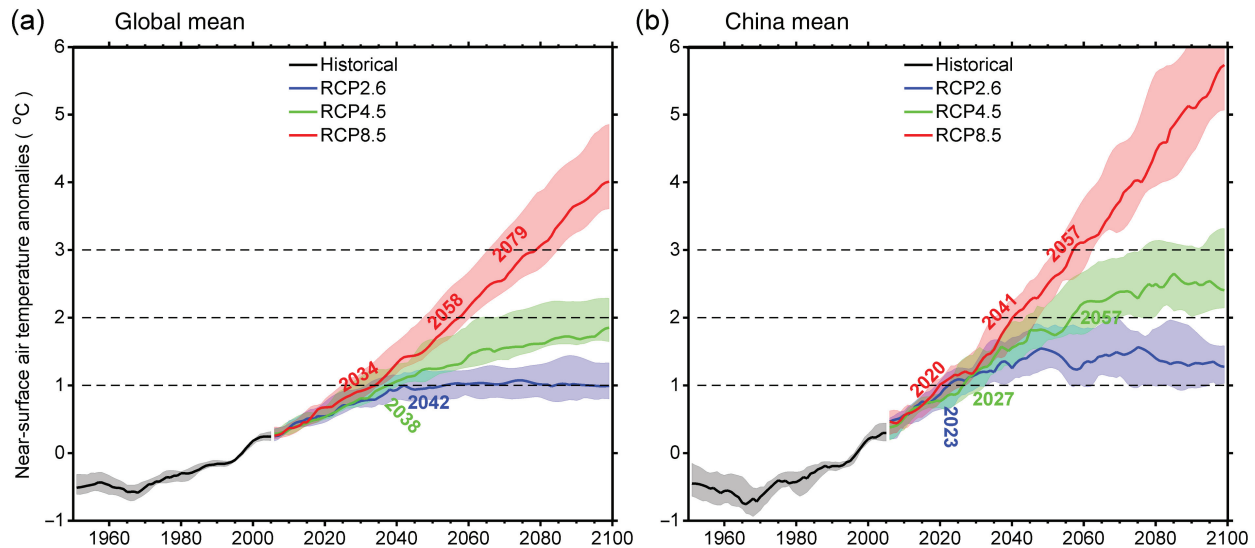


Figure 2. Annual mean temperature anomalies ($^{\circ}\text{C}$) relative to 1986–2005 in 19 CMIP5 models using RCP2.6, RCP4.5, and RCP8.5: (a) global mean, and (b) China mean. The temperature anomaly time series have been smoothed using an 11-year low-pass filtering method. The shading shows the interquartile model spread, i.e. the range between the 25th and 75th percentiles of the model ensemble to represent the confidence level, and the numbers in the figure are the years when the annual mean temperature increased by 1, 2, and 3°C . These years for China are generally considered to be the central points of the 20-year climatic means that are used for the difference calculations for each extreme index in this study.

4. Changes in climate extremes

4.1. Climate extreme changes at a warming of 1, 2, and 3°C

4.1.1. Extreme temperature events

Among the 27 ETCCDI indices (Table 2), there are 16 extreme temperature indices calculated from the daily minimum and maximum of near-surface temperatures (TN and TX, respectively). Figure 3 shows the median ensemble changes of five typical extreme temperature indices at the time of warming by 1, 2, and 3°C with respect to the 1986–2005 period in different RCPs in China, including the hottest and coldest days of the year (TXx and TNn), FD, SU, and growing season length (GSL). The changes are presented for all three of the RCPs at the 1°C level but only for RCP4.5 and 8.5 at the 2°C level and only for RCP8.5 at the 3°C level. The differences between 1, 2, and 3°C are obvious, as are some distinctions among the RCPs. At 1°C , there is model agreement for a lack of significance across some regions of China. At 2°C , there are many more regions exhibiting significant anomalies, with all the models agreeing on the direction of change in most cases. The progression from 2 to 3°C in RCP8.5 shows a further strengthening and extension of climate extreme changes. Taking TNn as an example, at the time of warming by 1°C , the temperature increase on the coldest nights shows a great difference over China, especially in Northeast China and the southern Tibetan Plateau, where the temperature increase is much larger in RCP4.5 and relatively smaller in RCP8.5. This phenomenon is closely associated with the different time-points when the models reach a temperature threshold of 1°C for the different scenarios. Furthermore, the temperatures on the coldest nights are observed to significantly increase, with the largest increase in China at

the time of warming by 3°C , then at 2°C , and relatively smaller at 1°C .

Relative to 1986–2005, there is a general increase in the annual maximum of TX and the annual minimum of TN over China at the different temperature-increase levels. The multi-model median increases in TXx and TNn are projected to be much larger than the increase in the mean temperature. Furthermore, the increase in TNn is generally much greater than that in TXx for the RCPs, particularly in the high-latitude and high-altitude regions in China, such as Northeast China, Xinjiang, and some regions of Tibet. The changes in the spatially weighted averages of TXx and TNn projected for the mean temperature increase of 1°C are 1.10 and 1.05°C in RCP2.6, 1.19 and 1.22°C in RCP4.5, and 1.11 and 1.12°C in RCP8.5, respectively. There is an approximately linear increase at the 2 and 3°C levels, which is similar to the pattern at the 1°C level. For example, the ensemble mean in RCP8.5 undergoes a 3.12 and 3.59°C increase for TXx and TNn, respectively, when the China mean temperature increases by 3°C (Table 2). All the models show consistent changes with the median ensembles of these two climate extreme indices for all the RCPs at the different temperature levels. However, the total variance due to inter-model and internal variabilities presents a similar magnitude as the change signals but with more spatial inhomogeneity (Figure 4). For TXx, the total variance is large in eastern and Northwest China but small in Tibet, and it increases with the mean temperature increase, mainly due to the inter-model variability amplification with time. The total variance of TNn is much larger than that of TXx but has similar spatial features for all the temperature levels. The large increase signal but small variance of TXx and TNn imply a credible future warming of the hottest day and the coldest day of the year in some regions of Tibet.

Table 2. Simple introduction to the 27 ETCCDI indices and their associated changes at the timing of warming by 1, 2, and 3 °C as calculated from the median ensemble means in China.

Label	Index name	Units	RCP2.6	RCP4.5			RCP8.5		
			1 °C (2023)	1 °C (2027)	2 °C (2057)	1 °C (2020)	2 °C (2041)	3 °C (2057)	
TXx	Max TX	°C	1.10 (100)	1.19 (100)	2.18 (100)	1.11 (100)	2.12 (100)	3.12 (100)	
TXn	Min TX	°C	0.80 (100)	1.08 (100)	2.09 (100)	0.91 (100)	1.88 (100)	3.09 (100)	
TNx	Max TN	°C	0.98 (100)	1.04 (100)	2.07 (100)	0.96 (100)	1.88 (100)	2.94 (100)	
TNn	Min TN	°C	1.05 (100)	1.22 (100)	2.39 (100)	1.12 (100)	2.18 (100)	3.59 (100)	
FD	Frost days	Days	-8.10 (100)	-9.00 (100)	-17.62 (100)	-9.13 (100)	-17.40 (100)	-26.86 (100)	
ID	Ice days	Days	-6.70 (100)	-7.39 (100)	-15.22 (100)	-7.10 (100)	-14.40 (100)	-20.90 (100)	
SU	Summer days	Days	7.88 (100)	9.48 (100)	19.39 (100)	8.27 (100)	17.71 (100)	25.64 (100)	
TR	Tropical nights	Days	6.16 (100)	6.72 (100)	14.53 (100)	6.73 (100)	13.11 (100)	19.89 (100)	
GSL	Growing season length	Days	9.14 (100)	10.31 (100)	20.16 (100)	9.34 (100)	19.45 (100)	28.32 (100)	
DTR	Diurnal temperature range	°C	-0.03 (74)	-0.01 (68)	0.02 (53)	-0.06 (79)	-0.06 (63)	-0.05 (68)	
TN10p	Cold nights	%	-3.25 (100)	-3.78 (100)	-5.64 (100)	-3.44 (100)	-5.47 (100)	-6.66 (100)	
TX10p	Cold days	%	-3.00 (100)	-3.11 (100)	-4.87 (100)	-2.93 (100)	-4.82 (100)	-6.13 (100)	
TN90p	Warm nights	%	9.30 (100)	10.93 (100)	22.27 (100)	9.94 (100)	21.80 (100)	33.64 (100)	
TX90p	Warm days	%	7.16 (100)	8.72 (100)	17.86 (100)	7.60 (100)	17.37 (100)	25.03 (100)	
WSDI	Warm spell duration index	Days	11.16 (100)	14.03 (100)	34.51 (100)	13.52 (100)	32.38 (100)	57.76 (100)	
CSDI	Cold spell duration index	Days	-2.00 (100)	-2.12 (100)	-3.14 (100)	-1.99 (100)	-2.97 (100)	-3.27 (100)	
RX1day	Maximum 1 day precipitation	mm	1.55 (100)	2.10 (100)	3.43 (100)	1.56 (100)	3.42 (100)	5.28 (100)	
RX5day	Maximum 5 day precipitation	mm	2.39 (100)	4.12 (95)	6.76 (100)	2.45 (95)	5.80 (100)	10.56 (100)	
SDII	Simple daily precipitation	mm	0.16 (100)	0.16 (100)	0.41 (100)	0.12 (95)	0.34 (100)	0.52 (100)	
R1mm	Number of wet days	Days	1.36 (74)	0.45 (58)	1.41 (74)	0.05 (53)	0.79 (63)	2.52 (74)	
R10mm	Heavy precipitation days	Days	0.57 (84)	0.54 (84)	1.98 (100)	0.43 (79)	1.32 (95)	2.27 (95)	
R20mm	Very heavy precipitation days	Days	0.32 (89)	0.42 (100)	0.94 (100)	0.26 (89)	0.76 (100)	1.19 (100)	
CDD	Consecutive dry days	Days	-0.66 (79)	-0.77 (63)	-1.14 (68)	-0.72 (79)	-1.66 (68)	-1.88 (74)	
CWD	Consecutive wet days	Days	0.08 (53)	0.06 (58)	0.13 (53)	-0.10 (58)	-0.06 (53)	0.12 (53)	
R95p	Very wet days	mm	17.45 (100)	20.30 (100)	44.24 (100)	15.73 (100)	36.05 (100)	56.90 (100)	
R99p	Extremely wet days	mm	9.64 (100)	12.33 (100)	24.39 (100)	10.80 (100)	20.84 (100)	34.22 (100)	
PRCPTOT	Total wet-day precipitation	mm	17.94 (89)	18.08 (95)	60.94 (100)	14.66 (84)	38.78 (100)	68.07 (95)	

The years of temperature increases by 1, 2, and 3 °C are shown in parentheses, which are generally taken to be the central points of the 20-year climatology for the calculation of the difference for each ETCCDI index with respect to 1986–2005. Model agreement refers to the number of models that show the same direction of change as the median ensemble mean, with its associated percentages of significant models that show the same direction of change in brackets (units: %) as depicted in IPCC reports. The projected changes in this table are shown in absolute terms relative to the reference period. Note that there are 19 models in Table 1 that were used for analyses in this study.

With the mean temperature increase, the number of FD (Figure 3) and ID (Figure S1, Supporting Information) are projected to significantly decrease in China, while the number of SU (Figure 3) and TR (Figure S1) increase. FD and ID particularly decrease in the Tibetan Plateau, but this decrease is accompanied with a relatively large variance (Figure 4). The decrease is strongest in RCP8.5 with reductions of more than 12 FD and 8 ID in most regions of China at the time of warming by 3 °C. The regions of southern China are also projected to experience a significant decrease in ID under all three of the RCPs, but the reduction magnitude is much smaller than in the northern regions of China. Considering China as a whole, all the models project reductions in both FD and ID in the three scenarios of warming of 1, 2, and 3 °C. FD

decreases by more than 8 days and ID decreases by more than 6 days even in the lowest forcing scenario RCP2.6 (Table 2). The numbers of SU and TR increase the most (>30 days) in some regions of eastern China, particularly based on RCP8.5 with a warming of 3 °C. However, the total variance is generally larger where the values are significantly increased. Increases are relatively small in SU and TR in Tibet, concurrent with less variance (Figure 4). The median ensembles of the spatially weighted averages report increases by as many as 7 days in SU and 6 days in TR in China when the temperature in China increases by 1 °C in RCP2.6. There are approximately linear increases in SU and TR with the increases in temperature and radiative forcing, and these factors are projected to increase by more as 25 and 19 days, respectively, under a warming of

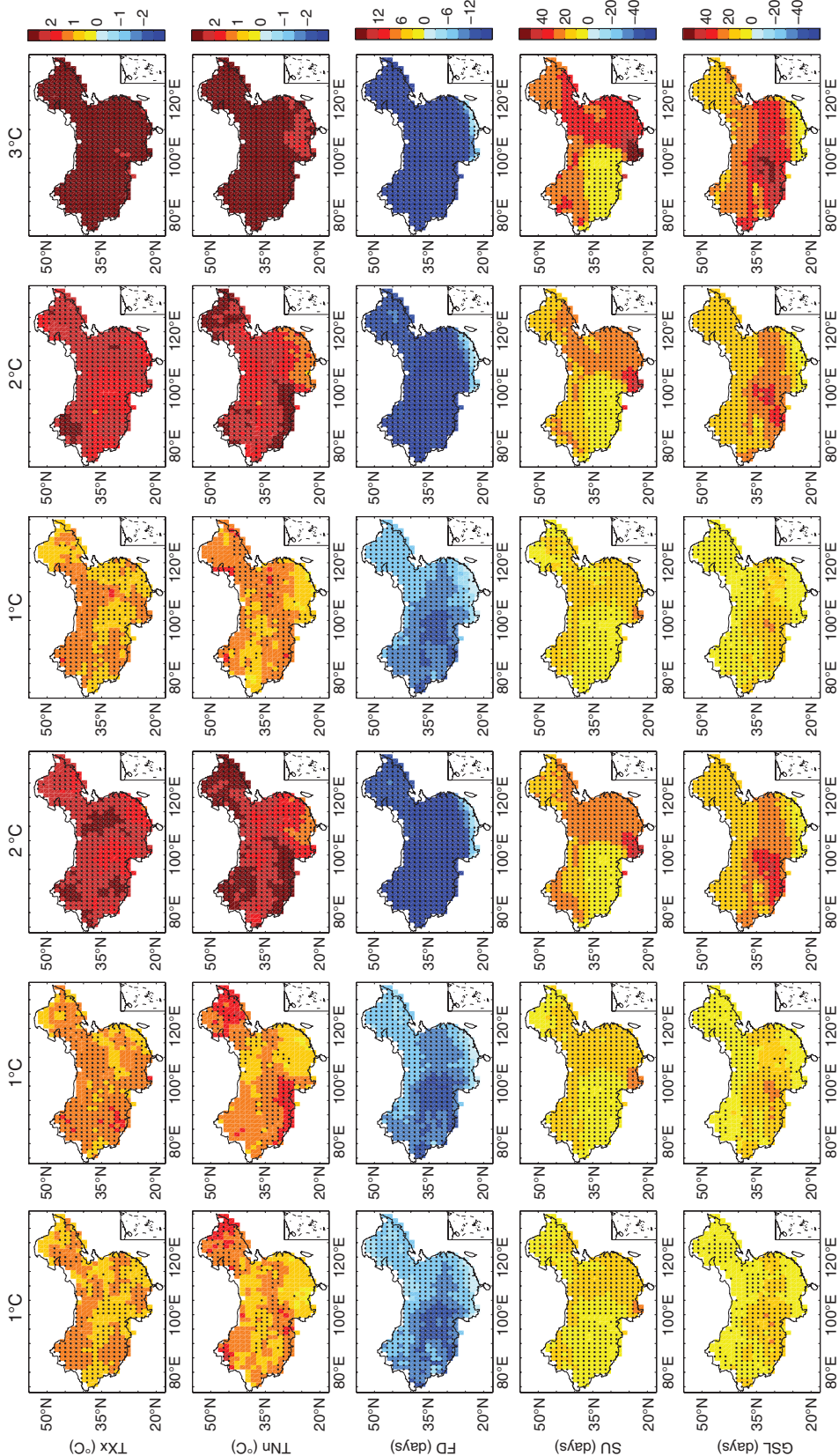


Figure 3. The multi-model median of extreme temperature changes in the maximum of TX (TX_x, top first row), the minimum of TN (TN_n, top second row), number of FD (middle row), number of SU (second row from bottom up), and GSL (bottom row) associated with warming in China, in the RCP2.6 (first column), RCP4.5 (next 2 columns), and RCP8.5 (last 3 columns) scenarios. Colour shading is applied only for the grids where 66% of the models agree on the direction of the change; stippling is shown for regions where at least 90% of all the models agree on the sign of the change.

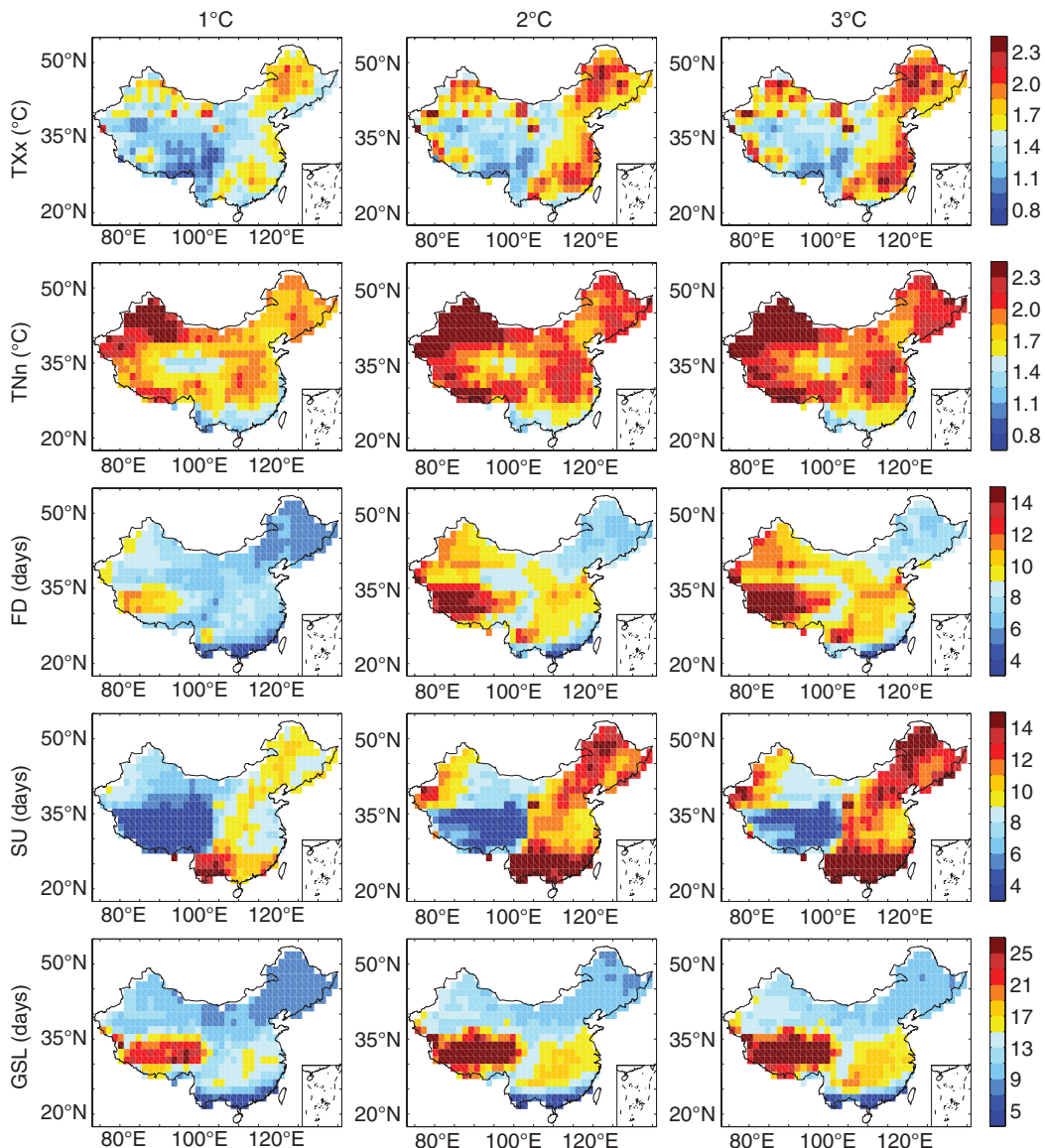


Figure 4. Maps of the total variance that represents the uncertainty of the projected climate extreme changes (TXx, TNn, FD, SU, and GSL) associated with warming within China of 1, 2, and 3 °C. Here, the total variance includes only internal variability and inter-model variability, not scenario variability, due to the different temperature-change levels for the different RCPs.

3 °C in RCP8.5 (Table 2). Although there is large variance mainly sourced from the inter-model difference, all the models used in this study show consistent increases with the median ensembles for both SU and TR. Considering the strong increases in these indices, China would experience increased heat stress if future climate change follows the paths of the studied RCPs, particularly RCP8.5.

Consistent with the mean temperature change, the GSL is projected to increase in all RCPs (Figure 3). This increase would be of great importance for increasing the agriculture production in China. Significant increases in GSL are observed throughout China and are most pronounced in the region of Tibet. Similarly, the changes increase with the mean temperature and as the radiative forcing increases. Relatively larger variance can be observed over Tibet compared with the other regions (Figure 4), but all the models show increases consistent

with the median ensemble change. The increase in GSL is up to 9 days at a warming of 1 °C and approximately 20 days at 2 °C. As the temperature increases by 3 °C in RCP8.5, the GSL increases by more than 28 days in China (Table 2).

We also analyse the projected changes in the percentile indices (Figure S2) represented by the exceedance rate (in %) relative to the 1961–1990 base period (Sillmann *et al.*, 2013), including cold nights (TN10p), cold days (TX10p), warm nights (TN90p), and warm days (TX90p). A consistent decrease can be observed in TN10p and TX10p from the reference period 1986–2005 to the 21st century at the different temperature-increase levels in all RCPs. In contrast, consistently significant increases can be observed in TN90p and TX90p in the future, and their increased magnitudes are much larger than those for TN10p and TX10p, exceeding one order of magnitude in RCP8.5 at 3 °C. Large

total variance is generally concurrent with large change signals for these percentile indices, but the signals usually show significance in excess to their noise. The median ensemble results for the progression from 1 to 3 °C indicate that both TX10p and TN10p would decrease by approximately 3% to over 6% (Table 2). The increases in warm events are much more dramatic and significant. TX90p increases by approximately 7% at 1 °C, more than 17% at 2 °C, and more than 25% at 3 °C, which would be a twofold increase over the number in the reference period 1986–2005 (~10%). The increase rate of TN90p is even faster than TX90p, and the TN90p values would be three times more than the values in the reference period at 3 °C in RCP8.5 (Table 2). This result provides further strong evidence that China would face more heat events in the future, even under the least radiative forcing scenario (RCP2.6).

Two other important indices are the cold spell duration (CSDI) and the warm spell duration (WSDI), which are projected to decrease and increase, respectively, in all RCPs at the different temperature-increase levels (Figure S2). The CMIP5 multi-model median changes in these two indices are significant throughout China. The strongest increases in WSDI occur in the regions of western and southern China, and the largest decreases in CSDI generally occur over the regions where WSDI significantly increases. At 1 °C, the median CMIP5 models project a decrease in CSDI by approximately 2 days and by 3 days at 3 °C relative to 1986–2005. WSDI increases strongly by more than 10 days at 1 °C, more than 30 days at 2 °C, and more than 57 days at 3 °C (Table 2).

The projections of the temperature-related extreme events from the CMIP5 models show significant changes in China, as described above. According to the IPCC confidence levels, the occurrence of extremely warm events in China would very likely increase, and the occurrence of extreme cold events would very likely decrease; however, the variances – mainly from the differences among the models – are comparable with the change signals. The change in diurnal temperature range (DTR) is an exception; this factor shows a weak decrease in China with a relatively large inter-model variance.

4.1.2. Extreme precipitation events

Changes in the precipitation indices relative to 1986–2005 are also expressed in absolute terms. Figure 5 provides the projected change maps of precipitation-related extreme indices in China at the different temperature-increase levels in the three RCPs, including the total precipitation of wet days (PRCPTOT), simple daily intensity (SDII), very wet days (R95p), max 5-day precipitation (RX5day), and consecutive dry days (CDD). PRCPTOT increases significantly over large parts of China in all three of the RCPs at 1, 2, and 3 °C increases relative to the reference period. The greatest changes are projected in Northeast China, North China, and Tibet under the RCP8.5 scenario at 3 °C. The areas of projected likely decreases in PRCPTOT are mainly concentrated in Southwest China, implying that the recent dry conditions in this region would likely continue

if future climate change follows the paths of the RCPs, despite relatively larger uncertainty than that in the other regions (Figure 6). SDII is projected to increase in this region, indicating that Southwest China would experience fewer precipitation days in the future.

Spatially, some differences can be observed in the projected changes between the extreme precipitation events and PRCPTOT in the future. R95p as well as R20mm (very heavy precipitation days) increase over most of China, except for some parts of Southwest China with likely decreases at the 1 °C level (Figure S3). The models that reach 2 °C generally show further strengthening in the regions where R95p has been observed to increase at 1 °C; however, R95p in Southwest China starts to increase at 2 °C and is further strengthened at 3 °C. The contribution of very wet days to the annual total wet-day precipitation, which is relevant for societal impacts, generally increases throughout China, especially in RCP8.5 at 3 °C (figure not shown). Similar spatial changes can be observed in RX5day and RX1day (max 1-day precipitation). In particular, RX5day increases over all of China, and the greatest increases are projected over eastern and southwestern China when the temperature in China increases by 2 °C. Although there are relatively large differences in the models regarding the change signals in Southwest China, the projections reveal that there would be increased risks of extreme precipitation events and associated flash flooding in the future (Figure 5).

As depicted in Figure 5, the maximum number of CDD is projected to significantly decrease, but the maximum number of consecutive wet days (CWD; Figure S3) increase in the regions where an increase is generally observed in PRCPTOT. A decrease of CDD occurring in northern China concurrently with the increase of CWD indicates a mitigation of drought conditions in this region relative to the last century. In contrast, in South and Southwest China, CDD is projected to increase, whereas CWD decreases. Particularly in Southwest China, the increased CDD combined with the increased RX5day indicates an intensification of drought and flooding events in this region, despite the decreased total precipitation in the future. Furthermore, in contrast to the other extreme indices, the total variance of CDD is largest in the Xinjiang region and smallest in Southwest China.

Table 2 also displays a summary of the projected changes of the spatially weighted averages in extreme precipitation indices in the three studied RCPs at 1, 2, and 3 °C with respect to the period 1986–2005. In contrast to the strong model agreement regarding the sign of the changes in temperature-related extreme indices, there is a relatively larger model spread regarding the precipitation indices. However, the consistency is larger for the more extreme events than for the moderate events. For example, the model agreement for R20mm is generally much larger than that for R10mm (heavy precipitation days) or R1mm (number of wet days) in all RCPs.

Median ensembles show an increase in the precipitation-related wetness indices and a decrease in one dry index (CDD) in the future based on the changes in

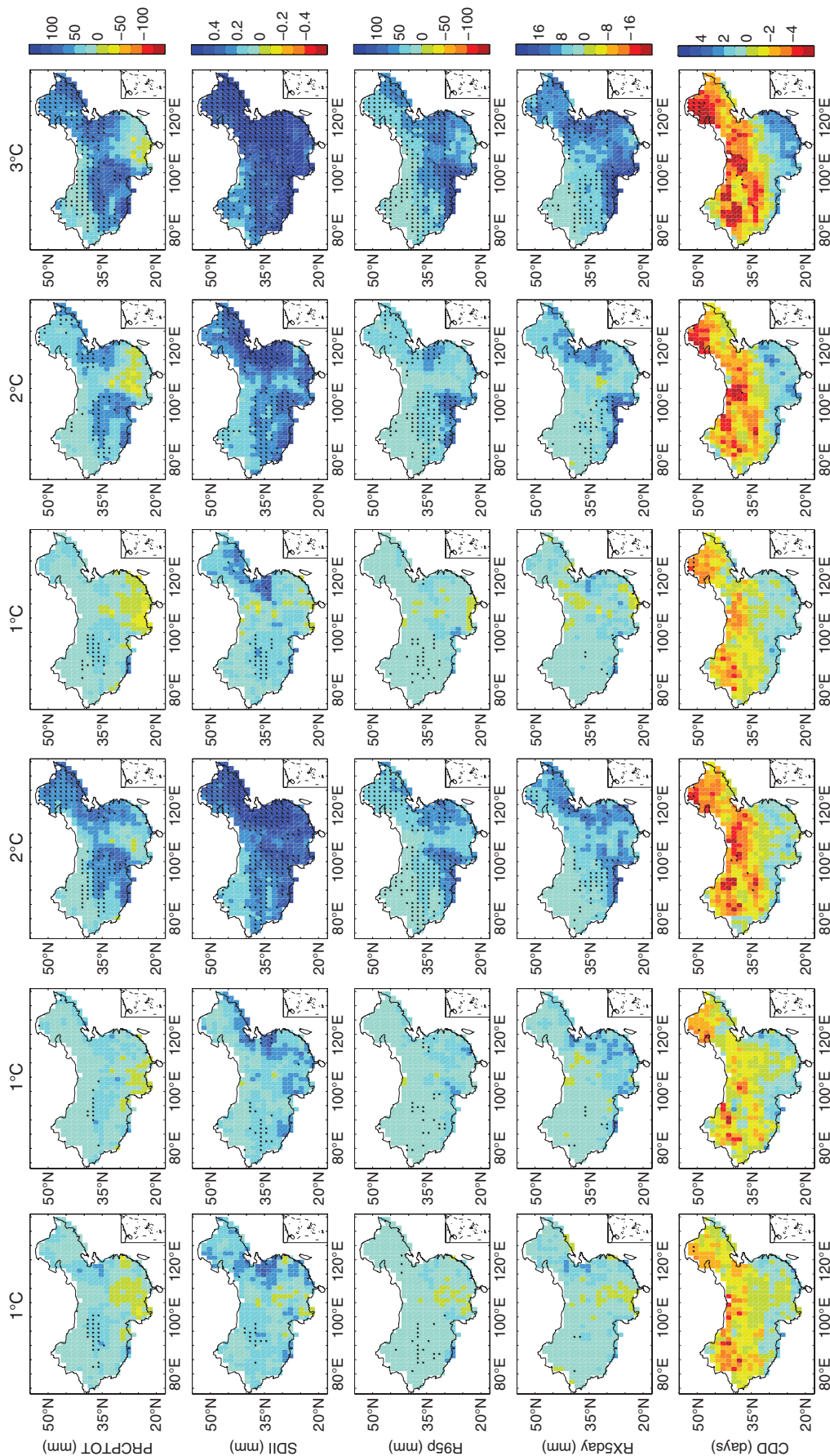


Figure 5. The multi-model median of changes of extreme precipitation events, including total precipitation of wet days (PRCPTOT), SDII, very wet days (R95p), maximum 5-day precipitation (RX5day), and CDD. Colour shading is applied only for the grids where 66% of the models agree on the direction of the change; stippling is shown for regions where at least 90% of all the models agree on the sign of the change.

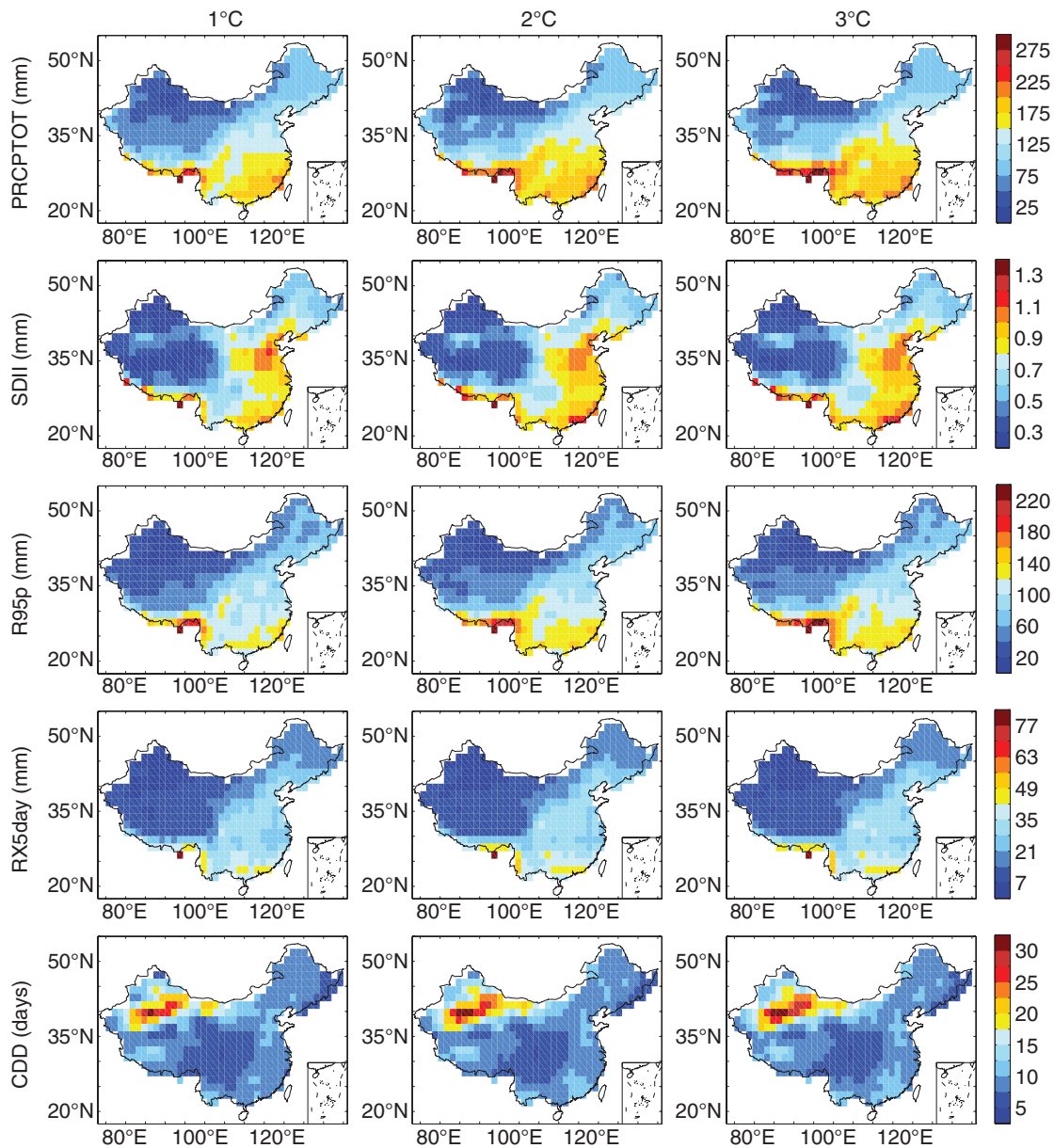


Figure 6. Maps of the total variance that represents the uncertainty of precipitation extreme events (PRCPTOT, SDII, R95p, RX5day, and CDD) associated with warming within China of 1, 2, and 3 °C. Here, the total variance includes only internal variability and inter-model variability, not scenario variability, due to the different temperature-change levels for the different RCPs..

the spatially weighted averages. At 1 °C, the total wet-day precipitation is projected to increase by approximately 15 mm, which is mainly driven by the significant increase of extreme precipitation (R95p) that also increases by approximately 15 mm. This action continues with the temperature increase, and R95p is projected to increase by approximately 57 mm at 3 °C concurrently with an approximately 68 mm increase in PRCPTOT. With the total precipitation increase, all models project an intensification of the daily precipitation intensity, and the daily precipitation events (RX1day) that do occur are likely to be more extreme. With the progression from 1 to 3 °C, SDII increases by 0.1 to 0.5 mm and RX1day increases by 1.6 to 5.3 mm in China in the RCP8.5 scenario. The days of R20mm and R10mm are also projected to consistently

increase; there would be one more day of R20mm and two more days of R10mm at the 3 °C level. RX5day, a valuable indicator of the risk of flooding, increases significantly with the warming in China, increasing by 2 mm at 1 °C, 4 mm at 2 °C, and 10 mm at 3 °C. The median CMIP5 projections for CDD and CWD diverge more substantially in China (Figures 5 and 6). For CDD, approximately two thirds of the models agree on the sign of the change at the different temperature-increase levels and different RCPs. CDD decreases by approximately half of a day in RCP2.6 at 1 °C and further to approximately 2 days in RCP8.5 at 3 °C. The changes in CWD are less consistent not only among the models but also among the scenarios. Only approximately half of the models project a weak increase in CWD at 1 °C in RCP2.6 and RCP4.5

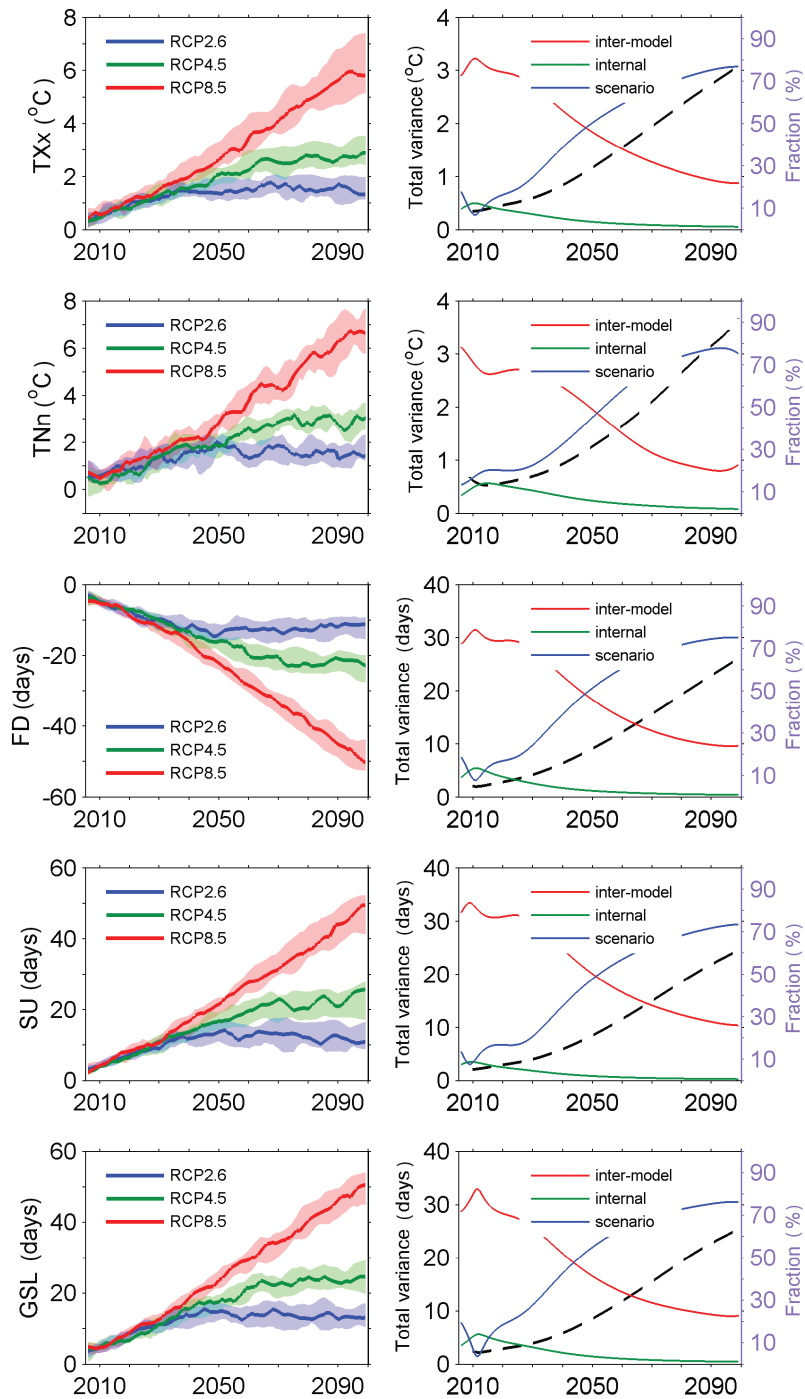


Figure 7. Spatially weighted averages of temperature extreme indices in China as simulated by the CMIP5 ensemble for RCP2.6 (blue), RCP4.5 (green), and RCP8.5 (red) displayed as anomalies from 1986 to 2005 in the left column. The solid lines indicate the ensemble medians, and the shading indicates the interquartile ensemble spread (25th and 75th quartiles). The time series are smoothed with an 11-year low-pass filter. The right column shows the corresponding evolutions of total variance (black line) and the fractions of its three sources (the blue line corresponds to the uncertainty from the scenario, the green line corresponds to internal variability, and the red line corresponds to inter-model variability).

but a weak decrease in RCP8.5. Opposite signs can also be seen at 2°C between RCP4.5 and RCP8.5. At 3°C , CWD shows a weak increase by approximately 0.1 days in RCP8.5, but the result is not robust.

From the above analysis, the results generally indicate an intensification of precipitation-related extreme events in China in the future. Most parts of China would likely experience more intensified extreme precipitation events

and increased risks of flooding. Concurrently, the dry conditions in northern China would be likely mitigated, making the region more suitable for rainfed agriculture. However, the occurrence risks of both drought and flooding events would likely increase in Southwest China, despite the decreased total precipitation in the future. That is, the dry conditions of recent years would continue and even be exacerbated with the warming in this region. Of

course, more evidence is needed in the future for further identification.

4.2. Temporal evolution of climate extremes

The rigorous science underpinning climate assessments requires evidence of future climate changes over time. Thus, the regionally averaged temporal evolutions of climate extreme indices are analysed here to further identify the climate change under a dangerous warming level. The model agreement is assessed as the interquartile model spread, i.e. the range between the 25th and 75th quartiles, for each RCP. The quantification of projection uncertainty from three sources and their contributions to the total variance are also discussed to further understand future climate changes in China.

Figure 7 illustrates the temporal evolution of five typical temperature indices with respect to 1986–2005 and their corresponding evolutions of total variances, as well as the ratios from the inter-model, internal, and scenario variabilities. Relative to 1986–2005, there are general increases in TXx and TNn. However, TNn is much more sensitive to warming than TXx, especially in the RCP8.5 scenario. In addition, the number of warm events, such as SU, TR, TX90p, and TN90p, is projected to significantly increase over time, along with GSL and WSDI. In contrast, the number of cold events, such as FD, ID, TX10p, and TN10p, shows a significant decreasing trend. These changes in temperature indices always increase with the intensification of radiative forcing, becoming much larger in RCP8.5 and smaller in RCP2.6.

The interquartile model spread indicates large differences among the projection changes of the temperature indices for each RCP, and the spread is reported to significantly increase over time. However, the scenario spread increases much more dramatically than that of the models and is much larger than that of the models for all temperature indices. This point is clear in the further investigation of the evolution of projection uncertainty sources (right column in Figure 7). Generally, the total uncertainty, defined as the total variance from the three sources, is projected to significantly increase with time, and different roles can be observed for the three sources in the increase of total variance. For the first decade of the 21st century, the uncertainty of the projection changes is mainly derived from the differences among the models, which can account for approximately 70% of the total variance, but the scenario-based and internal variabilities show almost the same roles. However, scenario variability increases much faster than inter-model variability over time, leading to an approximately 70% contribution from the scenario difference and less than 30% from the inter-model variability at the end of the 21st century. The role of internal variability is small or even negligible for the uncertainty of projection changes in temperature extremes compared with the other two sources. This result shows much similarity with the uncertainty discussion regarding the mean temperature change on the global scale (Hawkins and Sutton, 2009).

We also analyse the temporal evolutions of precipitation-related extreme changes in the future. Figure 8 presents the cases of five typical precipitation indices. PRCPTOT is projected to significantly increase over time, with the largest trend in RCP8.5 and the smallest in RCP2.6. A consistent pattern is observed in the evolutions of the other wet indices, including SDII, R95p, RX1day, RX5day, and R20mm. Consistent decreasing trends can be observed in the dry duration index of CDD; however, a discrepancy is seen in the projected changes of CWD (figure not shown), with a decreasing trend in RCP8.5 but increases in RCP2.6 and RCP4.5.

The projection uncertainty sources of all precipitation indices for China show significant increases with time. Similarly, the inter-model variability is the first source of the total variance in the first decade of the 21st century, followed by the internal and scenario variabilities, but the role of internal variability is somewhat larger than that of the scenario. However, by the end of the 21st century, there are some discrepancies in the performance of the uncertainty sources for the three indices [CDD in Figure 8, CWD, and R1mm (figures not shown)] compared with the other precipitation indices. For these three indices, the inter-model variability is still the dominant source of total variance (accounting for ~80% of the total variance), and the other two sources play relatively weak roles, but the scenario variability is projected to increase over time. For the other precipitation indices, the contribution of scenario variability shows a significant increase, accounting for approximately 60% of the total variance at the end of the 21st century. In contrast, the contribution of inter-model variability is projected to decrease and can account for approximately 30% of the total variance. This result corroborates that of a previous study focusing on the mean precipitation changes on the global scale (Hawkins and Sutton, 2011).

Briefly, the warm extremes in China are projected to significantly increase, while cold events significantly decrease under warming scenarios. Furthermore, there would be more frequent and severe precipitation extremes in the future. Of course, large uncertainty can be observed with these projections, and this uncertainty generally increases with time. For the first decades of this century, the uncertainty is mainly sourced from the inter-model variability, which generally accounts for approximately 70% of the variance. However, with the more rapid increase of scenario variability, the contribution of the inter-model variability is observed to decrease, and the scenario variability can explain approximately 60–70% of the total variance at the end of this century.

5. Discussion and conclusion

Based on the radiative forcing scenarios RCP2.6, RCP4.5, and RCP8.5, a number of CMIP5 climate models have been used to project anthropogenic climate change over the 21st century. The changes in climate extreme events defined by ETCCDI are analysed here at the timing of warming by 1, 2, and 3 °C in China, using a multi-model

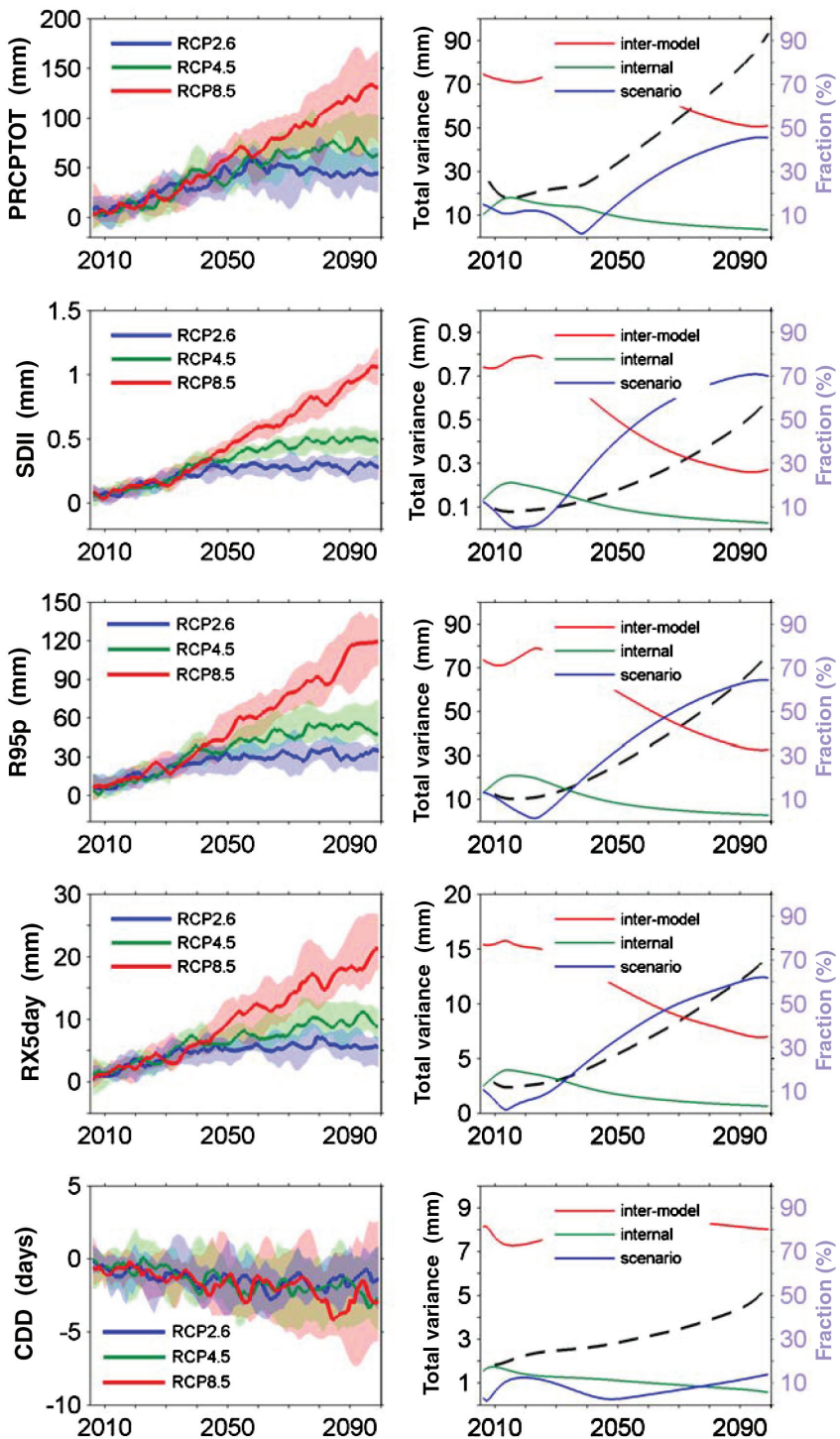


Figure 8. Spatially weighted averages of precipitation extreme indices in China as simulated by the CMIP5 ensemble for RCP2.6 (blue), RCP4.5 (green), and RCP8.5 (red) displayed as anomalies from 1986 to 2005 in the left column. The solid lines indicate the ensemble medians, and the shading indicates the interquartile ensemble spread (25th and 75th quartiles). The time series are smoothed with an 11-year low-pass filter. The right column shows the corresponding evolutions of total variance (black line) and the fractions of its three sources (the blue line corresponds to the uncertainty from the scenario, the green line corresponds to internal variability, and the red line corresponds to inter-model variability).

median ensemble projection. In addition, a simple discussion to the uncertainty is also attached to these projections.

A significant warming greater than the global average is projected over China by the CMIP5 models, indicating more vulnerability of society and ecosystems by regional warming. Thus, the projected changes in the spatial and temporal characteristics of climate extremes

are analysed as a function of the regional temperature increase in China in this study. The results generally indicate high model agreement of the projected changes in temperature-based indices at the different temperature levels, but the precipitation-based indices projections show more variation among the models in both the amplitude and direction of changes. Furthermore, the results show

relatively small change signals in climate extreme events in China at 1 °C, then larger anomalies at 2 °C, and further strengthening and extension at 3 °C.

For temperature-based indices, the changes in indices based on daily minimum temperature are generally more pronounced than those in indices based on daily maximum temperature. For example, the change in degrees of the coldest days (TN_n) of a year is projected to be much greater than that of the hottest days (TX_x) over most parts of China for each temperature level and each RCP. With increasing temperature, warm events in China, including SU, TR, TX90p, and TN90p, are projected to significantly increase, with the largest degree of change in RCP8.5 and the smallest in RCP2.6. In contrast, the frequencies of cold events, such as FD, ID, TX10p, and TN10p, show obvious decreases in the future. In addition, the duration of warm events is reported to increase rapidly, while the cold spell duration is obviously reduced. Thus, a tendency towards more warm events but fewer cold events in China in the future is very likely.

The changes in precipitation-based indices indicate that extreme precipitation increases much faster than PRCPTOT. A profound increase in very wet days (R95p) is generally observed along with an increase in R20mm in most regions in China. The risks of flooding events are reported to significantly increase in most regions, and the dry conditions in northern China are mitigated in the future. Among the regions considered, Southwest China particular stands out, not only with an intensification of dry conditions represented by CDD but also with an increased risk of flooding occurrence as described by RX5day. Furthermore, slight increases in R95p and RX1day suggest that precipitation would likely be much more extreme if it occurred, although dry conditions will become more severe in this region in the future.

It should be realized that uncertainty always surrounds these projections, mainly stemming from inter-model, scenario, and internal climate-system variabilities and other sources. The quantification analysis shows a relatively large contribution to the total uncertainty from the differences among the scenarios, followed by inter-model variability, in the projections of climate extreme events at the end of the 21st century. The role of internal variability is small or even negligible for the projections. However, high model agreement can be observed for the projected extreme changes, and such changes are considered to be very likely in most regions of China according to the IPCC confidence level.

This study is a stark reminder that climate change will very likely make the occurrence of climate extreme events more frequent and more extreme. Some impacts will be devastating, including the unprecedented heat waves, exacerbated water scarcity, and irreversible losses of biodiversity. Of course, some might argue that rising temperature may increase yields of grain crops due to the increase in GSL; however, this effect is unlikely. The impacts of such devastating drought or flood events on the yields cannot be offset by the increased GSL. For example, wheat yields are reported to decrease by 14–25%, maize yields decrease by

19–34%, and soybean yields decrease by 15–30% when the temperature increases by 1.8°–2.8 °C (Deryng *et al.*, 2011). The fact of warming cannot be disputed, and identifying how to mitigate its impact is a most urgent but difficult task at present. The solutions cannot lie only in climate finance or climate projects; effective risk management is the best choice. Thus, efforts investigating extremes, variability, and impacts associated with warming should be redoubled to support the development of effective adaptive measures. This study provides a framework for such analysis.

Nevertheless, from the temporal evolution of climate extreme changes, we also note that the change patterns of climate extremes show consistent trends with the evolution of CO₂ concentration under different radiative forcing scenarios. For example, the CO₂ concentration peaks at approximately 400 ppm around the mid-21st century and then declines to approximately 330 ppm by the end of the 21st century in RCP2.6. This characteristic change of CO₂ concentration has been well reflected by the temporal evolutions of climate extreme indices in China in RCP2.6. Similar cases can also be observed in RCP4.5 and RCP8.5. This result would mean that the climate extreme changes on a regional scale are sensitive to the CO₂ evolution. That is, human activities play a great role in the future climate extreme changes, inducing the extremes to be more frequent, stronger, and longer. Thus, reasonable limitations on greenhouse gas emissions and other human activities are necessary to mitigate climate deterioration. More sensitive analyses are needed regarding this aspect in the future.

Acknowledgements

We sincerely acknowledge the two anonymous reviewers whose kind and valuable comments greatly improved the manuscript. This research was jointly supported by the National Basic Research Program of China (Grant No. 2012CB955401), National Natural Science Foundation of China (Grant No. 41305061), the ‘Strategic Priority Research Program-Climate Change: Carbon Budget and Relevant Issues’ of the Chinese Academy of Sciences (XDA05090306), and the CAS-CSIRO Cooperative Research Program (GJGZ1223).

Supporting Information

The following supporting information is available as part of the online article:

Figure S1. The multi-model median of extreme temperature changes in the minimum of TX (TX_n, top first row), the maximum of TN (TN_x, top second row), number of ice days (ID, middle row), number of tropical nights (TR, second row from bottom up), and diurnal temperature range (DTR, bottom row) associated with warming in China, in the RCP2.6 (first column), RCP4.5 (next two columns), and RCP8.5 (last three columns) scenarios. Colour shading is applied only for the grids where 66% of the models

agree on the direction of the change; stippling is shown for regions where at least 90% of all the models agree on the sign of the change.

Figure S2. The multi-model median of temperature-based percentile indices, including TN10p (cold nights), TX10p (cold days), TN90p (warm nights), TX90p (warm days), WSDI (warm spell duration), and CSDI (cold spell duration). Colour shading is applied only for the grids where 66% of the models agree on the direction of the change; stippling is shown for regions where at least 90% of all the models agree on the sign of the change.

Figure S3. The multi-model median of precipitation indices, including the rainfall amount in extremely wet days (R99p), max 1-day precipitation (RX1day), maximum number of consecutive wet days (CWD), very heavy precipitation days (R20mm), heavy precipitation days (R10mm), and number of wet days (R1mm). Colour shading is applied only for the grids where 66% of the models agree on the direction of the change; stippling is shown for regions where at least 90% of all the models agree on the sign of the change.

References

- Alexander L, Zhang X, Peterson T, Caesar J, Gleason B, Tank A, Haylock M, Collins D, Trewin B, Rahimzadeh F, Tagipour A, Kumar K, Revadekar J, Griffiths G, Vincent L, Stephenson D, Burn J, Aguilar E, Brunet M, Taylor M, New M, Zhai P, Rusticucci M, Vazquez-Aguirre J. 2006. Global observed changes in daily climate extremes of temperature and precipitation. *J. Geophys. Res.* **111**: D05109, doi: 10.1029/2005JD006290.
- Chen HP. 2013. Projected change in extreme rainfall events in China by the end of the 21st century using CMIP5 models. *Chin. Sci. Bull.* **58**(12): 1462–1472.
- Chen HP, Sun JQ. 2009. How the “best” models project the future precipitation change in China. *Adv. Atmos. Sci.* **26**: 773–782.
- Chen HP, Sun JQ. 2013. Projected change in East Asian summer monsoon precipitation under RCP scenario. *Meteorol. Atmos. Phys.* **121**: 55–77.
- Chen HP, Sun JQ, Chen XL, Zhou W. 2012. CGCM projections of heavy rainfall events in China. *Int. J. Climatol.* **32**: 441–450.
- Chen HP, Sun JQ, Chen XL. 2013. Future changes of drought and flood events in China under global warming scenario. *Atmos. Oceanic Sci. Lett.* **6**: 8–13.
- Chen HP, Sun JQ, Chen XL. 2014. Projection and uncertainty analysis of global precipitation-related extremes using CMIP5 models. *Int. J. Climatol.* **34**: 2730–2748, doi: 10.1002/joc.3871.
- Deryng D, Sacks WJ, Barford CC, Ramankutty N. 2011. Simulating the effects of climate and agricultural management practices on global crop yield. *Global Biogeochem. Cycles* **25**(2): 1–18.
- Donat MG, Alexander LV, Yang H, Durre I, Vose R, Dunn RJH, Willett KM, Aguilar E, Brunet M, Caesar J, Hewitson B, Jack C, Klein Tank AMG, Kruger AC, Marengo J, Peterson TC, Renom M, Oria Rojas C, Rusticucci M, Salinger J, Elrayah AS, Sekels SS, Srivastava AK, Trewin B, Villarroel C, Vincent LA, Zhai P, Zhang X, Kitching S. 2013. Updated analyses of temperature and precipitation extreme indices since the beginning of the twentieth century: the HadEX2 dataset. *J. Geophys. Res.* **118**: 2098–2118.
- Gao XJ, Zhao ZC, Ding YH, Huang RH, Filippo G. 2001. Climate change due to greenhouse effects in China as simulated by a regional climate model. *Adv. Atmos. Sci.* **18**(6): 1224–1230.
- Gao XJ, Zhao ZC, Filippo G. 2002. Changes of extreme events in regional climate simulations over East Asia. *Adv. Atmos. Sci.* **19**(5): 927–942.
- Gao XJ, Shi Y, Giorgi F. 2011. A high resolution simulation of climate change over China. *Sci. China Earth Sci.* **54**: 462–472.
- Gao XJ, Shi Y, Zhang D, Giorgi F. 2012a. Climate change in China in the 21st century as simulated by a high resolution regional climate model. *Chinese Sci. Bull.* **57**: 1188–1195.
- Gao XJ, Shi Y, Zhang DF, Wu J, Giorgi F, Ji ZM, Wang YG. 2012b. Uncertainties of monsoon precipitation projection over China: results from two high resolution RCM simulations. *Clim. Res.* **52**: 213–226.
- Guivarch C, Hallegatte S. 2011. Existing infrastructure and the 2 °C target. *Clim. Change* **109**: 801–805.
- Hawkins E, Sutton R. 2009. The potential to narrow uncertainty in regional climate predictions. *Bull. Am. Meteorol. Soc.* **90**: 1095–1107.
- Hawkins E, Sutton R. 2011. The potential to narrow uncertainty in projections of regional precipitation change. *Clim. Dyn.* **37**: 407–418.
- IPCC. 2012. *Managing the Risks of Extreme Events and Disasters to Advance Climate Change Adaptation*. A Special Report of Working Groups I and II of the Intergovernmental Panel on Climate Change, Field CB, Barros V, Stocker TF, Qin D, Dokken DJ, Ebi KL, Mastrandrea MD, Mach KJ, Plattner GK, Allen SK, Tignor M, Midgley PM (eds). Cambridge University Press: Cambridge, UK, and New York, NY, 582 pp.
- IPCC. 2013. *Climate Change 2013: The Physical Science Basis*. Contribution of Working Group I to the Fifth Assessment Report of the Intergovernmental Panel on Climate Change, Stocker TF, Qin D, Plattner G-K, Tignor M, Allen SK, Boschung J, Nauels A, Xia Y, Bex V, Midgley PM (eds). Cambridge University Press: Cambridge, UK, and New York, NY, 1535 pp.
- James R, Washington R. 2013. Changes in African temperature and precipitation associated with degrees of global warming. *Clim. Change* **117**: 859–872.
- Jiang DB, Fu YH. 2012. Climate change over China with a 2 °C global warming. *Chin. J. Atmos. Sci.* **36**: 234–246 (in Chinese).
- Jiang DB, Tian ZP. 2013. East Asian monsoon change for the 21st century: results of CMIP3 and CMIP5 models. *Chin. Sci. Bull.* **58**: 1427–1435.
- Jiang DB, Wang HJ, Lang XM. 2005. Evaluation of East Asian climatology as simulated by seven coupled models. *Adv. Atmos. Sci.* **22**: 479–495.
- Jiang DB, Zhang Y, Sun JQ. 2009. Ensemble projection of 1–3 °C warming in China. *Chin. Sci. Bull.* **54**: 3326–3334.
- Knutti R. 2008. Should we believe model predictions of future climate change? *Philos. Trans. R. Soc. A* **366**: 4647–4664.
- Knutti R, Allen MR, Friedlingstein P, Gregory JM, Hegerl GC, Meehl GA, Meinshausen M, Murphy JM, Plattner GK, Raper SCB, Stocker TF, Stott PA, Teng H, Wigley TLM. 2008. A review of uncertainties in global temperature projections over the twenty-first century. *J. Clim.* **21**: 2651–2663.
- Lang X, Sui Y. 2013. Changes in mean and extreme climates over China with a 2 °C global warming. *Chin. Sci. Bull.* **58**: 1453–1461.
- Lu RY, Fu YH. 2010. Intensification of East Asian summer rainfall interannual variability in the twenty-first century simulated by 12 CMIP3 coupled models. *J. Clim.* **23**: 3316–3331.
- Ma JH, Wang HJ, Zhang Y. 2012. Will boreal winter precipitation over China increase in the future? The AGCM simulation under summer ‘ice-free Arctic’ conditions. *Chin. Sci. Bull.* **57**: 921–926.
- Meehl GA, Covey C, Delworth T, Latif M, McAvaney B, Mitchell JFB, Stouffer RJ, Taylor KE. 2007. The WCRP CMIP3 multi-model dataset: a new era in climate change research. *Bull. Am. Meteorol. Soc.* **88**: 1383–1394.
- Meinshausen M, Meinshausen N, Hare W, Raper SCB, Frieler K, Knutti R, Frame DJ, Allen MR. 2009. Greenhouse gas emission targets for limiting global warming to 2 °C. *Nature* **458**: 1158–1163.
- Moss RH, Edmonds JA, Hibbard KA, Manning MR, Rose SK, van Vuuren DP, Carter TR, Emori S, Kainuma M, Kram T, Meehl GA, Mitchell JFB, Nakicenovic N, Riahi K, Smith SJ, Stouffer RJ, Thomson AM, Weyant JP, Wilbanks TJ. 2010. The next generation of scenarios for climate change research and assessment. *Nature* **463**: 747–756.
- Orlowsky B, Seneviratne SI. 2012. Global changes in extreme events: regional and seasonal dimension. *Clim. Change* **110**: 669–696.
- Rogelj J, Hare W, Lowe J, van Vuuren DP, Riahi K, Matthews B, Hanaoka T, Jiang K, Meinshausen M. 2011. Emission pathways consistent with a 2 °C global temperature limit. *Nat. Clim. Change* **1**: 413–418.
- Sillmann J, Kharin VV, Zwiers WF, Zhang X, Branaugh D. 2013. Climate extremes indices in the CMIP5 multimodel ensemble: Part 2. Future climate projections. *J. Geophys. Res.* **118**: 2473–2493.
- Sun JQ, Wang HJ, Yuan W, Chen HP. 2010. Spatial-temporal features of intense snowfall events in China and their possible change. *J. Geophys. Res.* **115**: D16110, doi: 10.1029/2009JD013541.
- Taylor KE, Stouffer RJ, Meehl GA. 2012. An overview of CMIP5 and the experiment design. *Bull. Am. Meteorol. Soc.* **93**: 485–498.
- van Vuuren DP, Stehfest E, den Elzen MGJ, Kram T, van Vliet J, Deetman S, Isaac M, Goldeijk K, Hof A, Mendoza Beltran A,

- Oostenrijk R, van Ruijven B. 2011. RCP2.6: exploring the possibility to keep global mean temperature increase below 2 °C. *Clim. Change* **109**: 95–116.
- Wang HJ, Sun JQ, Chen HP, Zhu YL, Zhang Y, Jiang DB, Lang XM, Fan K, Yu ET, Yang S. 2012. Extreme climate in China: facts, simulation and projection. *Meteorol. Z.* **21**: 279–304.
- World Bank Group. 2012. *Turn Down the Heat: Why a 4 °C Warmer World Must Be Avoided*. World Bank: Washington, DC, 106 pp.
- Xu CH, Xu Y. 2012a. The projection of temperature and precipitation over China under RCP scenarios using a CMIP5 multi-model ensemble. *Atmos. Oceanic Sci. Lett.* **5**: 527–533.
- Xu Y, Xu CH. 2012b. Preliminary assessment of simulations of climate changes over China by CMIP5 multi-models. *Atmos. Oceanic Sci. Lett.* **5**: 489–494.
- Xu CH, Shen XY, Xu Y. 2007. An analysis of climate change in East Asia by using the IPCC AR4 simulations(in Chinese). *Adv. Clim. Change Res.* **3**(5): 287–292.
- Xu Y, Xu CH, Gao XJ, Luo Y. 2009. Projected changes in temperature and precipitation extremes over the Yangtze River basin of China in the 21st century. *Quat. Int.* **208**(1–2): 44–52.
- Xu Y, Gao XJ, Giorgi F. 2010. Upgrades to the reliability ensemble averaging method for producing probabilistic climate change projections. *Clim. Res.* **41**: 61–81.
- Xu JY, Shi Y, Gao XJ, Giorgi F. 2013. Projected changes in climate extremes over China in the 21st century from a high resolution regional climate model (RegCM3). *Chin. Sci. Bull.* **58**(12): 1443–1452.
- Zhang Y. 2012. Projections of 2 °C warming over the globe and China under RCP4.5. *Atmos. Oceanic Sci. Lett.* **5**(6): 514–520.
- Zhang Y, Sun JQ. 2012. Model projection of precipitation minus evaporation over China. *Acta Meteorol. Sin.* **26**(3): 376–388.
- Zhang X, Alexander L, Hegerl GC, Jones P, Tank AK, Peterson TC, Trewin B, Zwiers FW. 2011. Indices for monitoring changes in extremes based on daily temperature and precipitation data. *WIREs Clim. Change* **2**: 851–870.